Reducing Corrosion of Carbon Steel in 1 M HCl using Expired Glibenclamide, a Sulfonylurea-Based Inhibitor

Samir Abd El Maksoud[1], Abd El Aziz Fouda[2], Haby Badawy[1,*]

[1] Chemistry Department, Faculty of Science, Port Said University, Port Said *42526*, Egypt.
[2] Department of Chemistry, Faculty of Science, Mansoura University, Mansoura 35516, Egypt.

* Correspondence author: habybadawy@gmail.com

_____

ABSTRACT

This study assesses the corrosion inhibitory impact of expired Glibenclamide medication on carbon steel (CS) degrading in 1 M HCl. To assess the corrosion rate, weight loss (WL) and electrochemical methods were employed. The weight loss technique results show that raising the concentration and temperature of glibenclamide improves inhibitory efficiency. The greatest inhibitory efficiency was 84.5% at 300 ppm and 318 K. The substance adsorbs on the CS surface according to the Temkin adsorption isotherm. Electrochemical methods used in this study included potentiodynamic polarization (PP), electrochemical impedance spectroscopy (EIS), and electrochemical frequency modulation (EFM). The addition of glibenclamide decreased the corrosion current density (i_{corr}) while marginally changing the corrosion potential, indicating that it is a mixed-type inhibitor. The addition of varying doses of glibenclamide to the corrosive medium reduces the double layer capacitance (C_{dl}) while increasing the charge transfer resistance (R_{ct}). Different surface characterization techniques were employed to assess the compound's influence on the CS surface, scanning electron microscopy (SEM), Fourier transform infrared spectroscopy (FT-IR), atomic force microscopy (AFM) and x-ray photoelectron spectroscopy (XPS), were employed. The results support the compound's adsorption onto the CS surface. The molecular inhibitory effect of glibenclamide is demonstrated via quantum chemical calculations and molecular simulations. The results showed that the estimated compound adsorbs to the carbon steel surface.

Key Words: Inhibition, Electrochemical, Carbon steel, Glibenclamide, HCl

_____

1. INTRODUCTION

Corrosion is a serious concern for a variety of industries, including transportation, oil and gas, construction, and aerospace. Its negative consequences include material degradation, structural failures, and safety concerns, which can have serious economic and environmental consequences [1-7]. Furthermore, conventional corrosion management methods frequently rely on the use of toxic and harmful chemicals, which pose significant threats to both human health and the environment [8–10]. As a result, there is an urgent need to produce long-lasting corrosion inhibitors that are efficient, cost-effective, and ecologically friendly [11]. Corrosion inhibitors originating from natural sources, such as plant extracts, essential oils, and natural polymers, have high potential for long-term corrosion prevention. These inhibitors have three significant advantages: they are non-toxic, biodegradable, and create little environmental damage. These inhibitors work by attaching to metal surfaces and producing protective

layers, which effectively resist corrosion [12–14]. Carbon steel is utilized in corrosive environments such as offshore oil, gas, and other industries due to its superior mechanical properties and corrosion resistance [15–17]. Corrosion inhibitors, used in low concentrations in acidic solutions, have emerged as an essential strategy for metal protection, with the goal of reducing corrosion of metallic components [18–20]. Sulfonylurea derivative inhibitors have garnered a lot of attention as one of the most fully investigated inhibitors in recent years due to their great performance. They have properties such as low toxicity, no unpleasant odor, and good thermal stability. The adsorption effectively prevents contact between corrosive media and metal surfaces, resulting in excellent corrosion inhibition performance [21–25]. Many drugs' have been investigated as corrosion inhibitors of steel [26-41].

The current research aims to evaluate expired Glibenclamide as a corrosion inhibitor for CS corrosion in 1.0 M HCl. This examination is conducted using WL. The effect of temperature on the corrosion rate of CS is carried out to determine the type of adsorption isotherms and to calculate the thermodynamic parameters of activation and adsorption processes. Electrochemical techniques used in this study were PP, EIS, and EFM. The surface examinations were conducted using AFM, SEM, EDX, FT-IR, and XPS analyses. Quantum-chemical study of the corrosion inhibition of CS in acidic solutions using expired Glibenclamide drug.
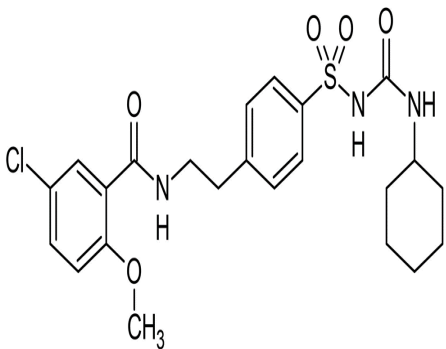
2. RESOURCES AND PROCEDURES

2.1 RESOURCES

Table 1 Chemical makeup percentage of CS employed in this study

Carbon	Manganese	Phosphorus	silicon	Chromium	Nickel	Sulfur	Copper	iron
0.14	0.52	0.05	0.02	0.03	0.02	0.04	0.02	rest

The degradative solution of 1.0 M, 35% hydrochloric acid utilized and 1000 ppm expired Glibenclamide drug stock solution was formulated, preferred doses (50–300 ppm) of inhibitor, Glibenclamide, for CS corrosion were determined by using different processes.

Table 2 the molecular configurations, nomenclature, chemical composition and molar mass of Glibenclamide

Configuration	Nomenclature	Molar Mass	chemical Composition
	Benzenecarboximidic acid, 5-chloro-N-[2-[4-[[[(E)-(cyclohexylimino)hydroxymethyl]amino]sulfonyl]phenyl]ethyl]-2-methoxy	493.143 Da	$C_{23}H_{28}ClN_3O_5S$

2.2. PROCEDURES

2.2.1 WEIGHT LOSS EXAMINATION

CS samples (7 pieces) each measuring (2 x 2 x 0.1 cm) employed, softened using sandpapers of varying grades (400–1200), until the metal sheets had a mirror-like finish. They were degreased with alcohol, rinsed by bidistilled water, dried and reweighed. Glibenclamide prepared in various concentration with one hundred milliliters hydrochloric acid of one molar concentration mixture prepared, another one prepared as blank, metal sheets then dipped in previous mixture for precise intervals (30, 60, 90, 120, 150 and 180 min.). After each interval, metal samples were removed from the solution, washed with bidistilled water, dried and reweighed.

Eq. (1) for inhibition efficiency (IE %) and surface coverage (θ) of Glibenclamide [42]:

$$IE\% = \left(1 - [\frac{W}{W_o}]\right) \times 100 \ = \theta \times 100 \tag{1}$$

W_o represent mass loss for CS without Glibenclamide and W represent mass loss for CS with Glibenclamide.

2.2.2 ELECTROCHEMICAL PROCEDURES

Potentiodynamic polarization, EIS, and EFM are employed in this study to identify CS corrosion, in a glass cell three electrodes were employed. Saturated calomel electrode, represent reference electrode, (1 cm^2) platinum sample represent a counter electrode, and (1 cm^2) CS sample represent a working electrode. Before each experiment, CS sample is softened using emery papers of varying grades then degreased and cleaned with bidistilled water then dried using filter papers, the open-circuit potential monitored for 30 min. and recorded till steady state reached.

2.2.2.1. P.P. PROCESSES

In this study plots of tafel were obtained by automatically varying the potential of electrode (E_{corr}) from – 0.750 to – 0.250 V, electrochemical current density of corrosion then determined.

From these measurements by Eq. (2), inhibition efficiency, surface coverage were then estimated [43]:

$$IE\% = \left(1 - [\frac{i_{corr(inh.)}}{i_{corr(blank)}}]\right) \times 100 \ = \theta \times 100 \tag{2}$$

$i_{corr\ (blank)}$ represent corrosion current densities without Glibenclamide, $i_{corr\ (inh)}$ with Glibenclamide

2.2.2.2. E.I.S. PROCESSES

Assessment of impedance were carried out in frequency range of 100 KHz to 0.1 Hz utilizing 5 mV amplitude. Eq. (3) calculated IE% and θ from (EIS) data [44]:

$$IE\% = \left(1 - [\frac{R°_{ct}}{R_{ct}}]\right) \times 100 \ = \theta \times 100 \tag{3}$$

The resistances to charge movement $R°_{ct}$ in absence of Glibenclamide plus resistances to charge movement R_{ct} in presence of Glibenclamide

Eq. (4) calculated capacitance of double layer (C_{dl}) measurements for varying concentration [45]:

$$C_{dl} = \frac{1}{2\pi \mathfrak{f}_{max} R_{ct}} \tag{4}$$

$\mathfrak{f}_{max}$ represent maximum frequency value.

2.2.2.3 EFM PROCESSES

EFM procedure represent rapid plus effective strategy for assessing the carbon steel (CS) degradation without needing to know the Tafel slopes. EFM was conducted with signal amplitudes of ten mV and two sine waves of two and five Hz. prominent one utilized for identify causality coefficients (CF-2 & CF-3), current density of corrosion (i_{corr}) and Tafel slope (βa & βc) [46].

2.2.3. SURFACE PROCESSES

Various analyses were conducted to survey the outer layer morphology of CS once exposure to degradative solution in addition with high concentration of Glibenclamide for a full day at 25°C. Surface roughness of the CS was assessed using atomic force microscopy (AFM), Thermo Fisher Nicolet IS10 (scanning probe microscope) was employed. The mass percentages of the surface components were determined using (SEM; JEOL JSM-5500, Japan), images taken at a magnification of x2000. XPS applied to identify the binding energies of various bonds discovered on CS surface, K-ALPHA (Thermo Fisher Scientific, USA) was used. FTIR spectra of pure solutions of Glibenclamide and CS using a PerkinElmer 1600 spectrophotometer.

2.2.4 SIMULATION PROCESSES

Quantum chemical indicators identified by MSD Mol440 were by applies density functional theory (DFT) [47], the calculated indicators for Glibenclamide included (σ) softness, (μ) molecular polarity, (X) electronegativity, (I) ionization potentials, (E_{LUMO}) lowest unfilled molecular orbital, (η) hardness, (ΔE) energy gap and (E_{HOMO}) highest filled molecular orbital.

3. FINDINGS AND ANALYSIS

3.1. MASS REDUCTION EXAMINATION

3.1.1. GLIBENCLAMIDE CONCENTRATION EFFECT

Figure 1 depicts the reduction of CS mass in an aggressive solution containing 1 M HCl in the absence and presence of various concentrations of Glibenclamide. Table 3 summarizes the mass loss data, the corrosion rate decreases and the inhibition efficiency decreases with the increasing of the inhibitor concentration [48]. Inhibition efficiency (IE %) for CS degradation was estimated using Eq. (1).
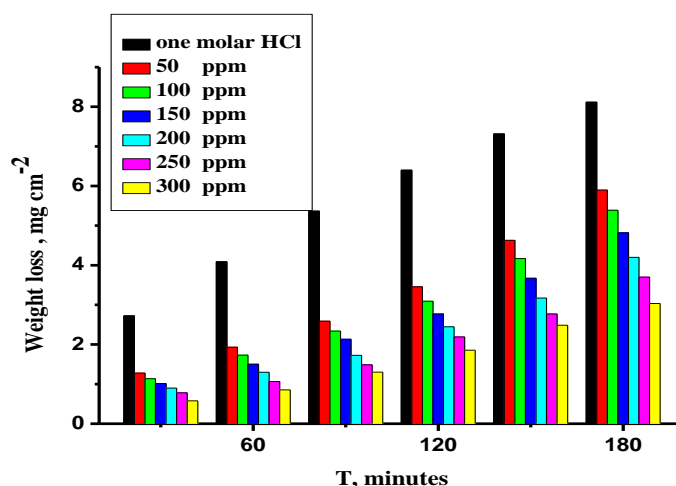
Figure 1 graphs mass reduction over time for degradation of CS in one molar hydrochloric acid, both in varying concentration of Glibenclamide and in its nonexistence

Table 3 values recorded from weight loss (WL) for carbon steel degradation at 120 min. in one molar hydrochloric acid, both in varying concentration of Glibenclamide and in its nonexistence

Concentration ppm	Temperature K	WL mg cm^{-2}	k_{corr}x10^{-3} mg cm^{-2} min^{-1}	Θ	% IE
Blank		6.4	53.33	-	-
50		3.08	25.64	0.519	51.9
100	298	2.85	23.76	0.554	55.4
150		2.56	21.36	0.599	59.9
200		2.38	19.82	0.628	62.8
250		2.16	17.97	0.663	66.3
300		2.06	17.17	0.677	67.7

3.1.2. TEMPERATURE EFFECT

Table 4 shows how the temperature influences the rate of CS breakdown in 1 M HCl, as well as various Glibenclamide dosages. According to the results, the corrosion rate increases rapidly with temperature. Figure 2 shows the variation of inhibition efficiency with the Glibenclamide dosages. The inhibition efficiency increases as the temperature increases. This indicates that Glibenclamide has a chemical adsorption on the CS surface [49].
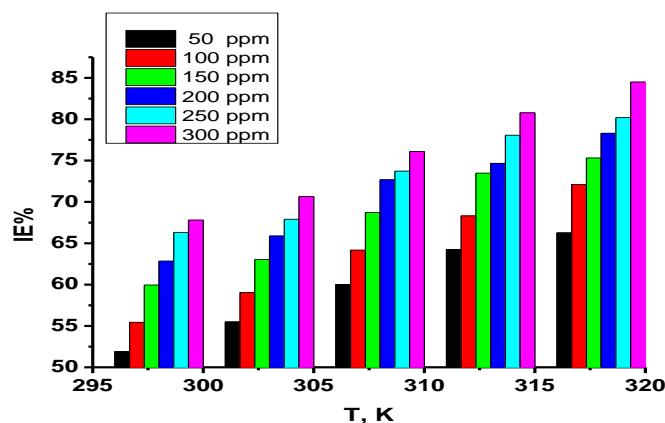
Figure 2 Graphs distinct temperature effect on IE% for CS in degradative acid solution at varied concentration of Glibenclamide.

Table 4 Weight loss (WL) values for carbon steel degradation post 120 min. in degradative acid both without plus with varying concentration of Glibenclamide at distinct temperature

Concentration ppm	Temperature K	WL, mg cm^{-2}	k_{corr}x10^{-3} mg cm^{-2} min^{-1}	θ	IE%
Blank		7.010	58.420	--------	-------
50		2.87	26	0.5549	55.49
100	303	2.87	23.92	0.5905	59.05
150		2.59	21.59	0.6302	63.02
200		2.39	19.93	0.6588	65.88
250		2.25	18.75	0.6790	67.90
300		2.08	17.25	0.7063	70.63
Blank		9.62	80.1	-	-
50		3.85	32.07	0.6001	60.01
100		3.45	28.74	0.6416	64.16
150	308	3.01	25.08	0.6872	68.72
200		2.63	21.91	0.7267	72.67
250		2.53	21.07	0.7372	73.72
300		2.29	19.16	0.7611	76.11
Blank		12.82	106.8	-	-
50		4.58	38.18	0.6426	64.26
100	313	4.06	33.85	0.6831	68.31
150		3.39	28.33	0.7347	73.47
200		3.25	27.06	0.7466	74.66
250		2.81	23.44	0.7806	78.06
300		2.46	20.53	0.8078	80.78
Blank		15.42	128.5	-	-
50		5.21	43.37	0.6625	66.25
100		4.30	35.85	0.7211	72.11
150		3.81	31.73	0.7531	75.31
200	318	3.35	27.89	0.7829	78.29
250		3.05	25.45	0.8020	80.20
300		2.54	20.92	0.8449	84.49

3.1.3. ACTIVATION THERMODYNAMIC PARAMETERS

The corrosion rate of the reaction is influenced by the temperature; Eq. (5) specifies this relation according to Arrhenius Eq. (5) [50-51]:

$$k_{corr} = A . \exp(-E_a / RT) \tag{5}$$

Where A is the Arrhenius constant, E_a represents the activation energy, T is the absolute temperature, and R is the gas constant. Figure 3 depicts a straight-line plot of log k_{corr} vs. 1/T; the slopes of the lines can be used to compute E_a. Table 5 shows the calculated and reported values for E_a. From the transition state theory, as indicated in Equation (6):

$$k_{corr} = RT/N h \exp \Delta S^* \exp -\Delta H^* / RT \tag{6}$$

In this equation, ΔS^* and ΔH^* represent the activation entropy and enthalpy. Figure 4 depicts a plot of log k_{corr}/T vs. 1/T, resulting in straight lines from their slopes. Table 5 shows the calculation and reporting of ΔH^*. The data show that the presence of an inhibitor leads to a drop in E_a values, indicating chemical adsorption. The positive values of ΔH^* indicate the endothermic activation process, which confirms the chemical adsorption of the investigated inhibitor on the CS surface [52]
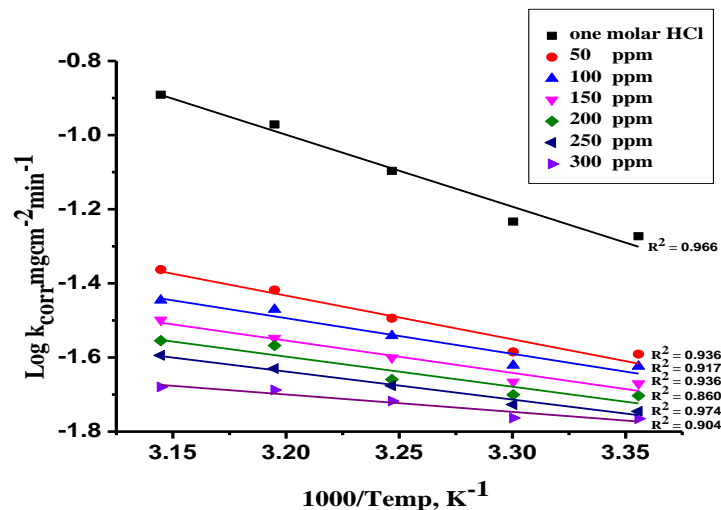

Figure 3 carbon steel degradation in degradative acid solution Arrhenius graph both without plus with Glibenclamide varying concentration at temperature ranging from (298-318K)
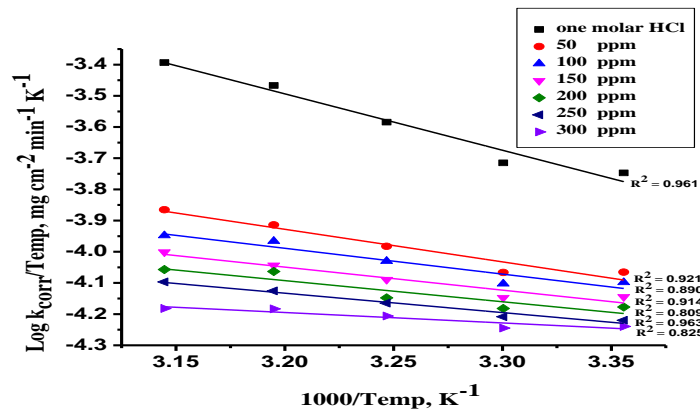

Figure 4 Carbon steel degradation in degradative acid solution transition state graph both without plus with Glibenclamide varying concentration at distinct temperature

Table 5 carbon steel degradation in degradative acid solution thermodynamic activation values both without plus with Glibenclamide varying concentration at temperature ranging from (298-318K)

Concentration ppm	E_a^*, kJ mol^{-1}	ΔH^*, kJ mol^{-1}	$-\Delta S^*$, J mol^{-1}K^{-1}
0	37.20	34.60	153.60
50	26.43	23.94	210.6
100	23.02	18.97	212.2
150	22.03	17.31	220.2
200	17.31	14.47	231.9
250	15.55	11.99	237.8
300	13.94	11.79	239.7

3.1.4. ADSORPTION ISOTHERMS

Adsorption of inhibitors on metal surfaces is controlled by metal characteristics and charge, inhibitor chemical structure, and electrolyte concentration [53]. Eq. (7) describes the Temkin isotherm and aligns well with the experimental data.

$$\theta = \left(\frac{2.303}{a}\right) \text{Log } K_{ads} + \left(\frac{2.303}{a}\right) \text{Log } C \tag{7}$$

Where Θ is the surface coverage, K_{ads} is the adsorption constant, C is the concentration, and "a" is the heterogeneous factor. Figure 5 shows the relation between Θ vs. log C. where a, K_{ads} and $\Delta G°_{ads}$ calculated and recorded in Table 6. Indicated the adsorption isotherm follows the Temkin model in a good manner.

$$\Delta G^o_{ads} = -RT \ln (55.5 \, K_{ads}) \tag{8}$$

Glibenclamide has a strong chemical adsorption on CS surfaces, with increasing $\Delta G°_{ads}$ approximately - 40 kJ.mol^{-1} .The adsorption process is spontaneous due to the negative value [54]. ($\Delta H°ads$) was calculated from Eq. (9) [55]:

$$\text{Log } K_{ads} = -\frac{\Delta H^o_{ads}}{2.303 \, RT} \tag{9}$$

Figure 6 represents the relation between log K_{ads} and 1/T. $\Delta H°_{ads}$ was calculated and recorded in table 6. ($\Delta S°_{ads}$) was calculated from Eq. (10).

$$\Delta G^o_{ads} = \Delta H^o_{ads} - T\Delta S^o_{ads} \tag{10}$$

A previous study found that higher values of ΔH (more than 40 kJ mol⁻¹) and ΔS (about 100 kJ mol⁻¹) indicate an endothermic and chemisorption process [56]. The presence of non-bonding electron pairs from Glibenclamide atoms suggests interactions with the CS surface. A positive "a" value implies that the adsorbed layers are involved with the carbon steel surface. Furthermore, the increase in K_{ads} with temperature shows that the adsorption equilibrium improves with higher temperatures.

The measured negative entropy values in Table 6 show that Glibenclamide is adsorption rather than desorption on the CS surface. Increasing ΔS°_{ads} values. [57]
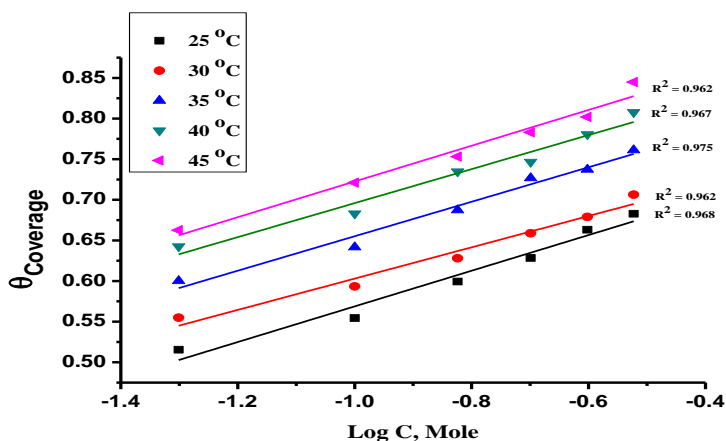

Figure 5 Glibenclamide adsorption onto carbon steel surface graphs θ versus Log C. at different temperature (298-318K)

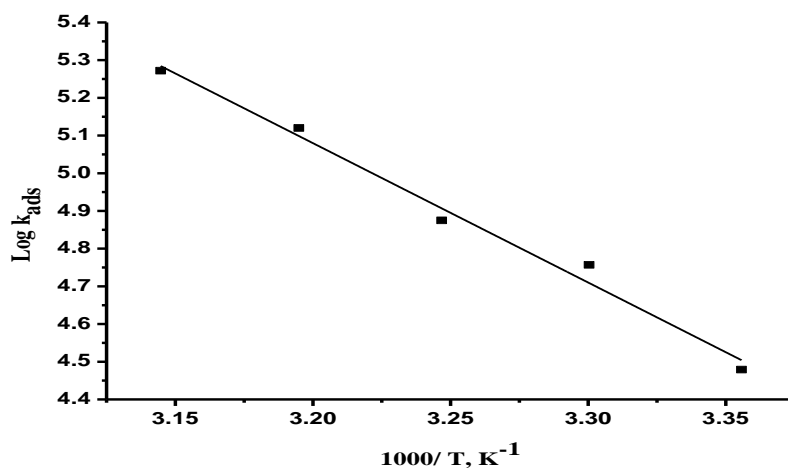**Figure 6 Glibenclamide varying concentration adsorption onto carbon steel surface graphs Log K_{ads} over 1/T at different temperature (298-318K)**

Table 6 Temkin isotherm adsorption data for Glibenclamide onto CS surface in degradative acid solution at distinct temperature

Temperature K	Log $K_{ads,}$ M^{-1}	A	$-\Delta G^{\circ}_{ads}$ kJ mol^{-1}	ΔH°_{ads} kJ mol^{-1}	$-\Delta S^{\circ}_{ads}$ J mol K^{-1}
298	4.479	12.1	35.5		119.3
303	4.757	12.7	38.1		126.1
308	4.875	13.5	38.4	53.7	125.1
313	5.120	13.6	41.1		131.6
318	5.272	15.0	49.8		140.7

3.2. ELECTROCHEMICAL PROCEDURES

3.2.1. P.P. PROCESSES

   CS polarization behavior in 1 M HCl in the absence and presence of varying concentrations of Glibenclamide is illustrated in figure 7. The electrochemical parameters are calculated and tabulated in Table 7. βa & βc denote to the anodic and cathodic Tafel slopes, E_{corr} is the corrosion potential, θ is the surface coverage, IE% is the inhibition efficiency and i_{corr} is the corrosion current density. The addition of Glibenclamide leads to a decrease in i_{corr} values, suggesting an effective corrosion inhibitor a mixed-type function of the inhibitor inferred from minimal changes observed in the Tafel slopes and E_{corr} [58].
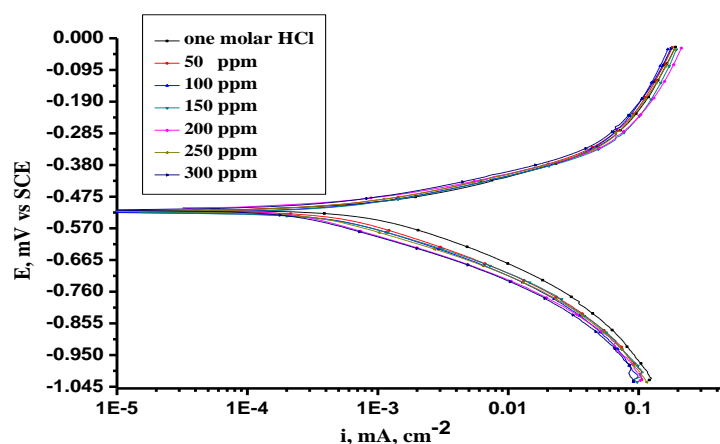
Figure 7 Carbon steel degradation in degradative acid solution potentiodynamic polarization graph with varying concentrations of Glibenclamide

Table 7 values from the potentiodynamic polarization of carbon steel in degradative acid solution, both without plus with Glibenclamide varying concentrations

Concentration ppm	- E_{corr}, mV vs. SCE	i_{corr}, µA cm^{-2}	-β_c mV dec^{-1}	β_a mV dec^{-1}	k_{corr}, mpy	θ	IE%
0	533	1480	210	134	755	----	----
50	517	495	187	112	263	0.665	66.5
100	521	420	173	94	220	0.716	71.6
150	522	381	168	91	198	0.742	74.2
200	511	341	155	85	187	0.769	76.9
250	518	307	164	80	159	0.792	79.2
300	515	272	160	75	141	0.816	81.6

3.2.2. E.I.S. PROCESSES

EIS is used to understand the electrochemical processes that occur on the CS surface in acid solution. Figure 8 depicts Nyquist plots of CS with and without different concentrations of the inhibitor in 1M HCl. They are semicircles that move along the real impedance of the x-axis. Metal surface heterogeneity and frequency dispersion can result in defective capacitance loops. The semicircle radii are modified by the inhibitor concentrations.

The widths of the capacitance loops are higher in the presence of the inhibitor than in the absence, indicating that inhibitor molecules can significantly promote the anticorrosion process of CS surface [59]. The concentration of inhibitor molecules adsorbing on the CS surface is proportional to their concentration. CPE [60-61] can be used to replicate the double-layer capacitance (C_{dl}) from Eqs. 11 and 12, where ω_{max} is the frequency that corresponds to the maximum value of the imaginary component of the Nyquist plot.

$$C_{dl} = Y_o (\omega_{max})^{n-1} \tag{11}$$

$$C_{dl} = \varepsilon\varepsilon_0 \left(\frac{A}{\delta}\right) \tag{12}$$

The correlated equivalent circuit used to model the CS/HCl interface is illustrated in Figure 9; Rs denotes the uncompensated solution resistance and R_{ct} denotes the charge transfer resistance (R_{ct}). Table 7 demonstrates that R_{ct} values rise as inhibitor concentration rises. The R_{ct} value varies from 41 to 116 Ω/cm2. This suggests that the inhibitor forms a protective coating on the electrode surface at all concentrations. As a result, corrosive ions are effectively prevented from coming into contact with the working electrode. At the same time, the addition of inhibitors reduces C_{dl} levels by establishing a protective layer on the steel surface. The inhibitor has the best inhibitory efficiency at a concentration of 300 ppm, according to the EIS technique.
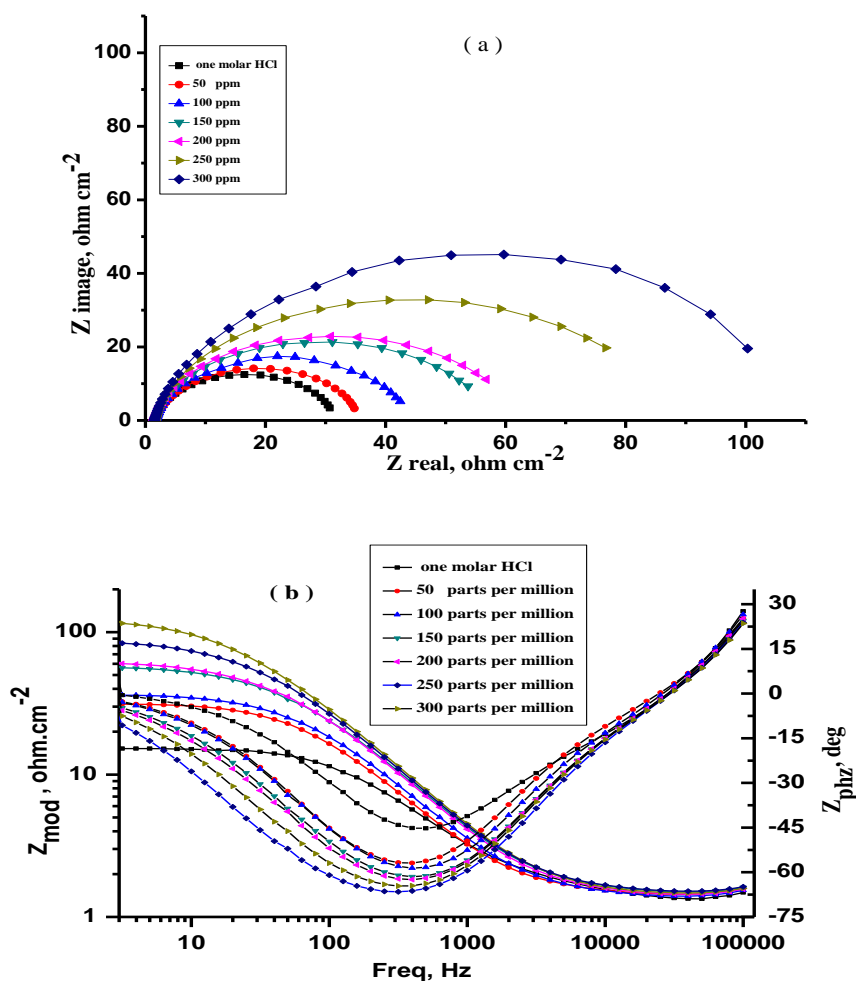
Figure 8 Carbon steel degradation in degradative acid solution EIS spectra, (a) Nyquist and (b) Bode graph both without plus with Glibenclamide varying concentrations
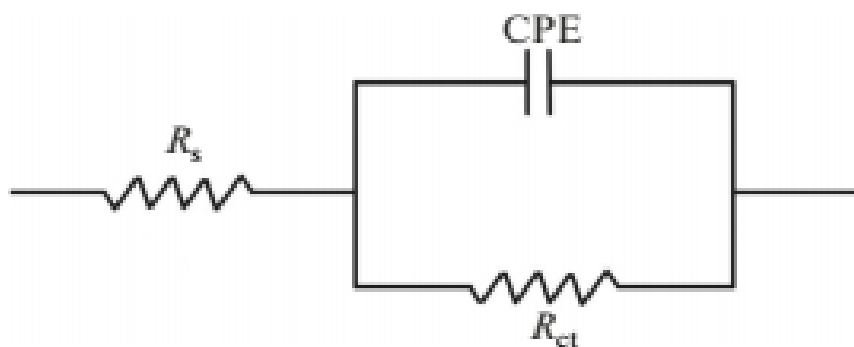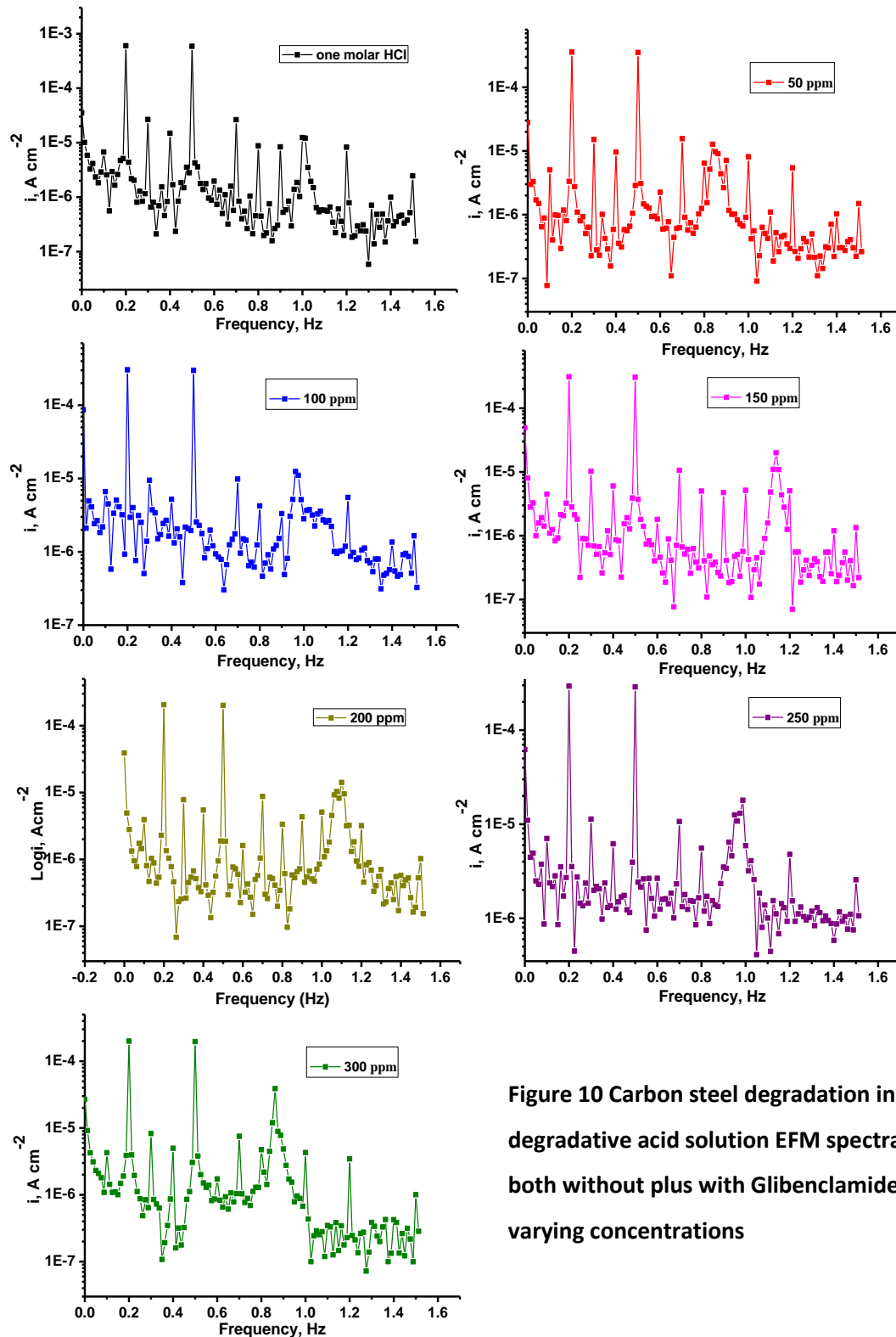

Figure 9 circuit model graph utilized for representing EIS measurements

Table 8 Carbon steel degradation in degradative acid solution EIS values both without plus with Glibenclamide varying concentrations

Concentration ppm	$R_s,$ cm^2	$Y_o,$ $\mu\Omega^{-1}s^n cm^{-2}$	n	$R_{ct},$ Ωcm^2	$C_{dl},$ $\mu F\ cm.^{-2}$	θ	IE%
0	1.90	325	0.970	29.0	284.40	---	---
50	1.8	259	0.842	41	110.4	0.292	29.2
100	1.6	243	0.835	48	100.8	0.395	39.5
150	1.2	216	0.827	55.6	85.6	0.478	47.8
200	1.4	209	0.812	62.5	76.5	0.536	53.6
250	1.9	192	0.801	89.8	70	0.677	67.7
300	1.8	186	0.794	116.9	69	0.751	75.1

3.2.3. EFM PROCESSES

For EFM measurements, two sine waves with frequencies of 2 and 5 Hz are applied to the cell in the absence and presence of various dosages of the investigated compound. The Tafel constants are not required because the results are generated instantly using this method [62]. The output current varies in frequency and is nonlinear. The causality factors (CF-2 and CF-3) obtained by EFM testing are important because they validate the EFM measurements if their values are close to the theoretical values (2 and 3). Harmonic peaks in the current's output spectrum undermine the data for CR. The higher the current density (i_{corr}), the greater the peaks. EFM spectra of CS in 1 M HCl in the absence and presence of different concentrations are shown in figure 10 and the results are shown in Table 9. As the inhibitor concentration rose, the i_{corr} decreased.

Figure 10 Carbon steel degradation in degradative acid solution EFM spectra both without plus with Glibenclamide varying concentrations

Table 9 Carbon steel degradation in degradative acid solution electrochemical values both without plus with Glibenclamide varying concentrations

Concentration ppm	i_{corr}, μAcm^{-2}	$-\beta_c$, $mV\ dec^{-1}$	β_a, $mV\ dec^{-1}$	CF-2	CF-3	k_{corr}, mpy	θ	IE%
0	929	191	135	1.8	3.5	480	-----	----
50	497	98	77	1.9	2	263.5	0.481	48.1
100	426.6	97	74	1.7	2.7	223.3	0.556	55.6
150	312.2	110	78	1.7	2.3	164.1	0.674	67.4
200	299.2	91	70	1.6	2.8	166.6	0.688	68.8
250	270.6	107	73	1.8	2.1	140.3	0.717	71.7
300	255	112	84	1.7	2	132.5	0.734	73.4

3.3. SURFACE PROCESSES

3.3.1. SEM PROCESSES

Carbon steel surface morphologies (SEM) after immersion in one molar hydrochloric acid, both with the highest concentration (300 ppm) and without the Glibenclamide (blank), for 24 hours at 298K. Figure 11 illustrates the surface damage and pitting in the degradative solution, which is significantly greater compared to the images obtained with Glibenclamide, development of a shielding layer on CS surface resulted in reduced damage and pitting observed with Glibenclamide that helps prevent metal degradation [63].
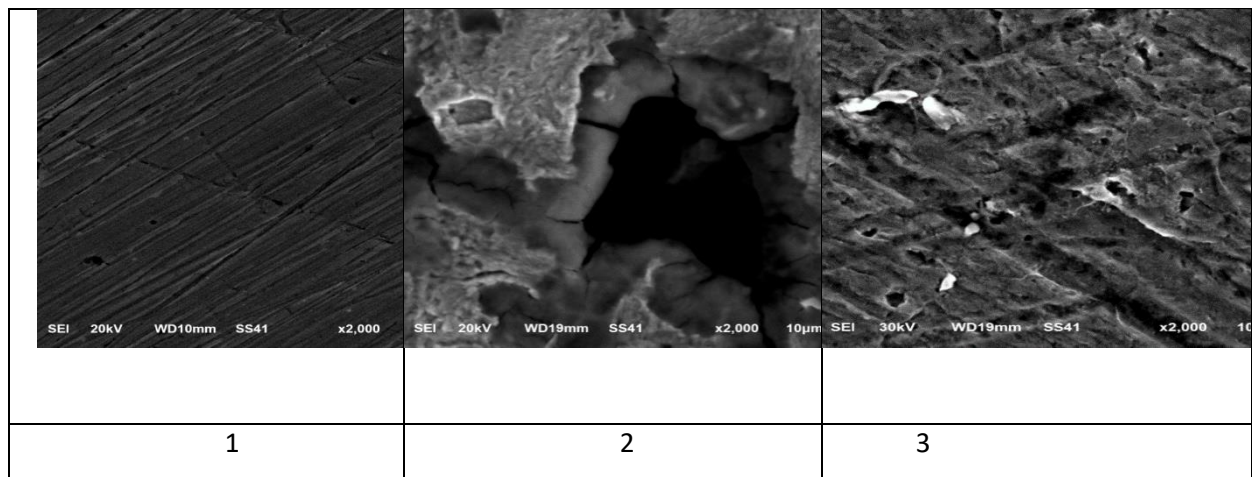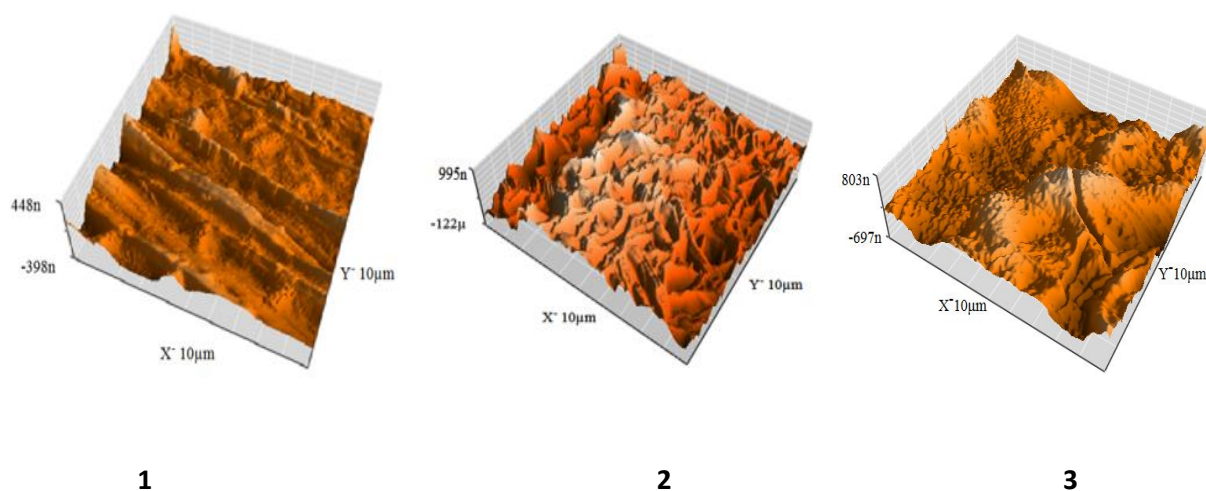

Figure 11 CS specimens SEM images: (1) uncontaminated CS, (2) CS immersed full day in degradative acid and (3) CS immersed full day in degradative acid plus Glibenclamide of optimal concentration

3.3.2. AFM PROCESSES

An ideal tool for examining surface topography, AFM and assess inhibition efficacy on CS after immersion in a degradative acid [64] because it provides nanoscale to microscale three-dimensional (3D) images of surfaces. Figure 12 displays the 3D AFM images of carbon steel degradation in a degradative acid, both without plus with 300 ppm Glibenclamide. The mean deviation of surface irregularities represented by (Rq), the typical variations across the entire texture measurements represented by (Ra). AFM of carbon steel in degradative solution alone show significant degradation and increased roughness. In contrast, the presence of Glibenclamide results in less pitting, suggesting development of the shielding film on CS external layer.

IE% record derived from electrochemical tests plus mass reduction test corroborate observed surface texture measurements. Consistency between roughness data illustrated in table 10. Indicated less textured surface of CS suggesting development of the shielding film formed by Glibenclamide.

1　　　　　　　　　　　　**2**　　　　　　　　　　　　**3**

Figure 12 CS specimens AFM scans: (1) before exposure to degradative solution, (2) immersed full day in degradative acid and (3) immersed full day in degradative acid plus Glibenclamide of optimal concentration

Table 10 CS specimens surface texture data involvement plus nonexistence of Glibenclamide optimal dose in one molar hydrochloric acid for one-day

samples	Mean surface texture	Surface root mean square texture
uncontaminated Carbon steel surface	48.7 nm	63.0 nm
Carbon steel + one molar hydrochloric acid(blank)	271.7 nm	335.6 nm
Carbon steel surface + one molar hydrochloric acid + Glibenclamide	180.7 nm	238.3 nm

3.3.3. FTIR PROCESSES

Strategy utilized for examining Glibenclamide functional groups adsorbed upon CS outer layer. Figure 13 shows IR spectral data of Glibenclamide and illustrates the development of the shielding film on CS external layer after 6-hour immersion in degradative acid plus an optimal Glibenclamide concentration 300 ppm. Examining the distinct peaks, minor changes are observed, with some functional group frequencies disappearing and others shifting as shown in table 11. These changes as a result of (chemisorption) where interrelation plus bonding of Glibenclamide with outer layer of carbon steel. Identified peaks indicate the presence of Glibenclamide, which includes heteroatoms serve as active sites protecting CS by forming a protective layer when exposed to a degradative solution on carbon steel [65-66] like O and N, as well as π electrons from double bonds.
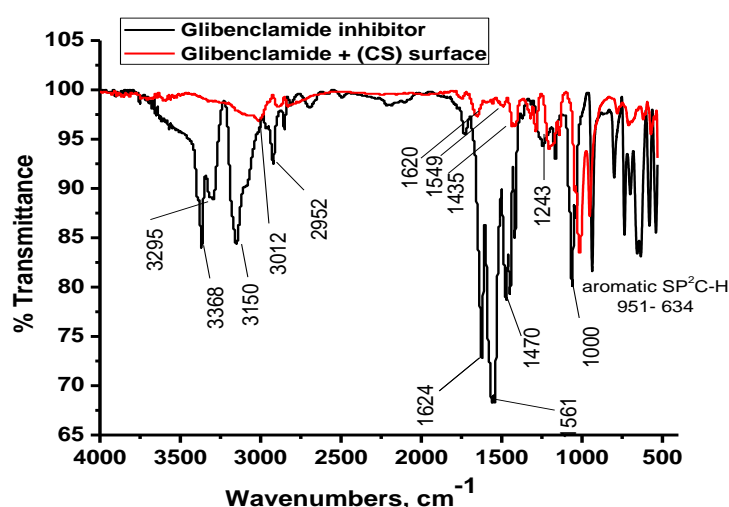

Figure 13 Glibenclamide FT-IR spectra alone and with carbon steel after a 6-hour immersion in one molar hydrochloric acid with an optimal Glibenclamide concentration 300 ppm.

Table 11 FT-IR analysis of Glibenclamide alone and with carbon steel after 6-hour immersion in one molar hydrochloric acid with an optimal Glibenclamide concentration 300 ppm.

Peak frequencies (cm^{-1})	Functional groups represented by frequencies	Peak shifts, frequency changes and new peaks (cm^{-1}) observed after adsorption
3368,3295	$-NH_2$ primary amine Stretching vibration	------
3150	SP^2 (-C-H) Stretching vibration	3012
2952	stretching SP^3 -C-H	------
1624	stretching aromatic conjugated (-C=O) in amide group	------
1561	-N-H- bending vibration	1598
1470	stretching (C=C)	1435
1243	Alkoxy aliphatic (C-O)	1205
1000	bending -C-N-	------
951-634	bending aromatic SP2 (C-H)	952-544
800	di-substituted in the ortho positions	781
735	di-substituted in the Para positions	710
650	di-substituted in the meta positions	620

3.3.4. XPS PROCESSES

Technique applied to gain deeper understanding of the chemical behavior for Glibenclamide upon the outer layer of CS. Figure 14 and 15 shows CS outer layer post immersed full day in a degradative acid plus Glibenclamide of optimal concentration Fe 2p, O 1s, Cl 2p, C 1s, and N 1s XPS profiles data. Following deconvolution by curve fitting. The complex forms observed in all XPS spectra were attributed to their corresponding species through a deconvolution fitting process [67–75]. Data analysis measurements reported at table 12. XPS spectrum verified that a protective film composed of C, O, and N atoms formed upon outer layer of CS by Glibenclamide.
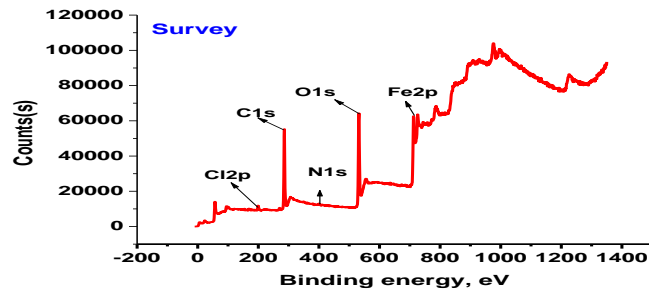
Figure 14: Glibenclamide optimal concentration adsorbed upon outer layer of CS XPS spectra in degradative acid
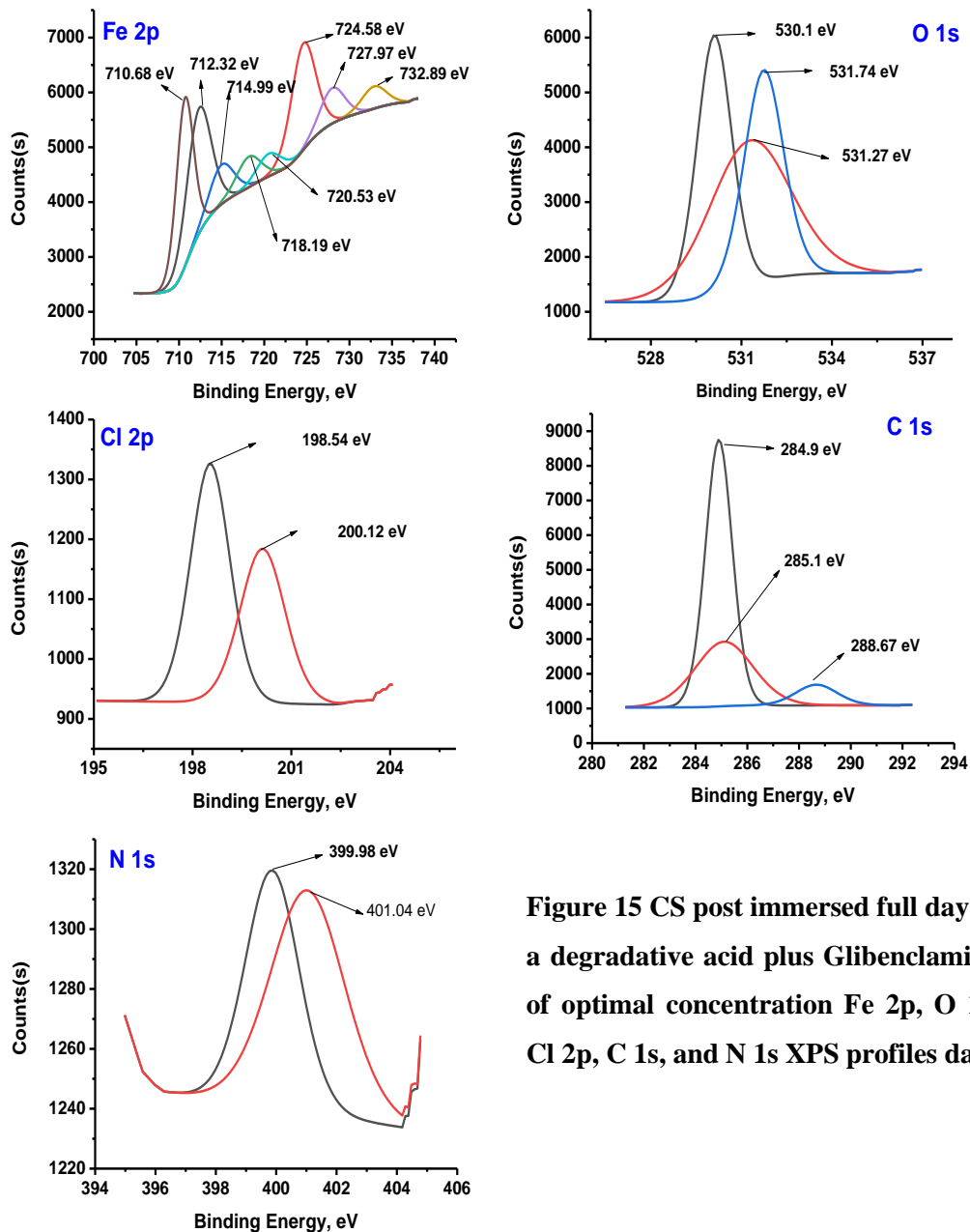

Figure 15 CS post immersed full day in a degradative acid plus Glibenclamide of optimal concentration Fe 2p, O 1s, Cl 2p, C 1s, and N 1s XPS profiles data

Table 12 predicted bonds related to various spectra binding energies lists.

Type of scan	Peaks value of binding energies (eV)	Predicted bonds
Fe 2p	710.68	2p3/2 core level electrons of iron in its +2 oxidation state as found in FeO
	712.32	2p3/2 core level electrons of iron in its +3 oxidation state as found in Fe_2O_3 or $FeCl_3$
	714.99	2p3/2 core level electrons of iron in its +2 oxidation state as additional peaks
	718.19	2p3/2 core level electrons of iron in its +3 oxidation state as additional peaks
		2p3/2 core level electrons of iron in its +3 oxidation state as additional peaks
	720.35	2p1/2 core level electrons of iron in its +2 oxidation state as found in FeO
	724.58	2p1/2 core level electrons of iron in its +3 oxidation state as found in Fe_2O_3
	727.97	2p1/2 core level electrons of iron in its +3 oxidation state as additional peaks
	732.89	
O 1s	530.01	Iron in its +3 oxidation state as found in Fe_2O_3
	531.27	Carbon-oxygen single bond
	531.74	Carbonyls shows up slightly higher in energy
Cl 2p	198.54	Chlorine atom in 2p3/2 orbital
	200.12	Chlorine atom in 2p1/2 orbital slightly higher energy
C 1s	284.5	Carbon atoms bonded to each other in aromatic ring
	285.1	Different carbon bonds with O, N or Cl
	288.67	Carbonyl carbon in amides or similar structures
N 1s	399.98	Imines or other similar compounds
	401.04	Nitrogen-hydrogen single bond

3.4. QUANTUM CHEMICAL AND STATISTICAL PARAMETERS

Quantum parameters, predict the relation between Glibenclamide molecular structure and its effectiveness against carbon steel degradation, significantly impact the electronic interaction between carbon steel and Glibenclamide solution. These parameters are presented in Table 13. Glibenclamide electron concentrations distributions shown in figure 16. Elevated E_{HOMO} values suggest a stronger propensity of Glibenclamide to transfer electrons to vacant d-orbitals of CS, ensure stronger adsorption. Conversely, a greater propensity for accepting electrons due to Lower E_{LUMO} values. ΔE indicates distribution of electron density plus molecules reactivity, molecular stability and reactivity indicated by data of (η) and (σ) [76] as listed in table 12. A higher softness (σ) and lower hardness (η) usually correlate with better inhibition efficiency. Glibenclamide polarity and electron-sharing bonding type represented by (μ), which affected by electron distribution. Generally, hard molecules with larger (ΔE) are more resistant to electronic perturbations, while soft molecules with smaller (ΔE) are more reactive and efficient in corrosion inhibition due to their ease of electron donation. Glibenclamide function as electron donor, while carbon steel with its vacant d-orbitals, function as electron acceptor [77].

inhibitor	Glibenclamide
Highest energy molecular orbital	
Lowest energy molecular orbital	
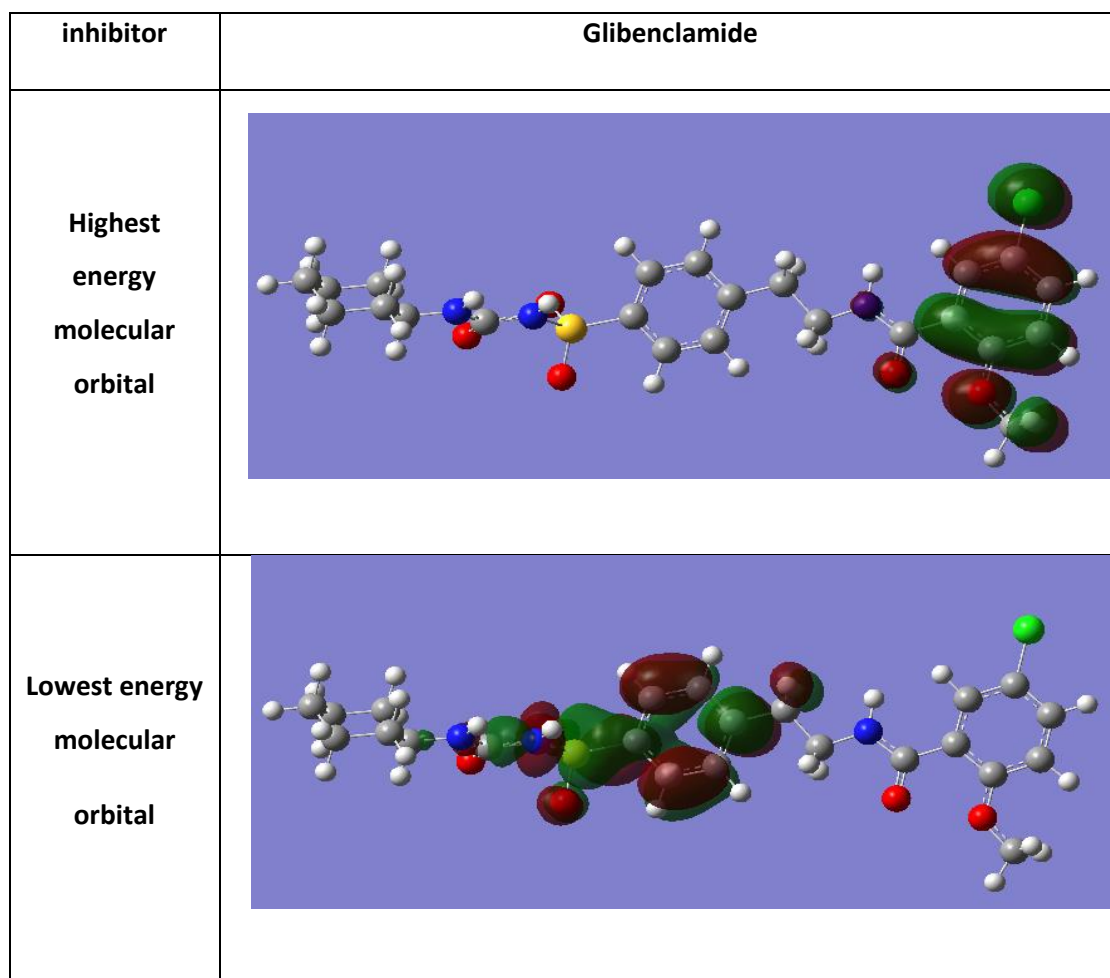
Figure 16 Glibenclamide highest energy molecular orbital plus lowest energy molecular orbital electronic densities distributions.

Table 12 Molecular quantum metrics for Glibenclamide in solution

| Metrics	E_{HOMO} (eV)	E_{LUMO} (eV)	ΔE (eV)	η (eV)	σ (eV)	Pi (Ev)	X (eV)	μ (Debye)
Glibenclamide	-6.294	-1.986	4.326	2.163	0.46	-4.14	4.14	10.76

4. MECHANISM OF INHIBITION

Adsorption of inhibitors on metal surfaces is influenced by many factors, such as the inhibitor's chemical structure, charge distribution, and surface type. Previous studies have demonstrated that the CS surface becomes positively charged when exposed to HCl solution [78-79]. As a result, the adsorption of hydrated chloride ions (Cl-) on the positively charged metal surface generates an excessive negative charge towards the solution side.

In the following stage, Glibenclamide occurs in HCl in its neutral form, which is in equilibrium with the protonated inhibitor form: Glibenclamide's neutral and protonated forms contain oxygen atoms inside functional groups (O-H, O-CH3, and SO2), sulphur and nitrogen atoms, and π-electrons in the aromatic ring, all of which are typical of corrosion inhibitors [80]. Consequently, the neutral and protonated forms of glibenclamide are most likely to interact with the CS in HCl solution, mostly via the following suggested mechanisms:

(a) Interaction between the CS surface atoms' unoccupied d-orbitals and the unshared electron pair of the Glibenclamide compound's nitrogen (N), sulfur (S), and oxygen (O) atoms.

(b) Donor-acceptor interactions between aromatic ring electrons and empty d-orbitals on CS surface atoms.

(c) Glibenclamide may benefit from electron migration from occupied CS surface atoms to anti-binding molecular orbitals (empty π^*). As previously demonstrated, organic inhibitor chemicals are easily protonated in acidic environments. This increases their adsorption on the steel surface through electrostatic interactions with previously deposited chloride ions (Cl-) on the positively charged CS surface.

This method relies on the first phase of the chemisorption process to maintain charge transfer between the inhibitor molecule and the metal surface Given the proposed mechanisms and results, it is reasonable to predict that chemisorption and electrostatic (physisorption) interactions will dominate in the adsorption processor of the examined molecule with the CS surface.Fig.17 displays a postulated corrosion inhibition mechanism for Glibenclamide CS in HCl media based on both experimental and computational investigations, as well as the above-mentioned analyses.
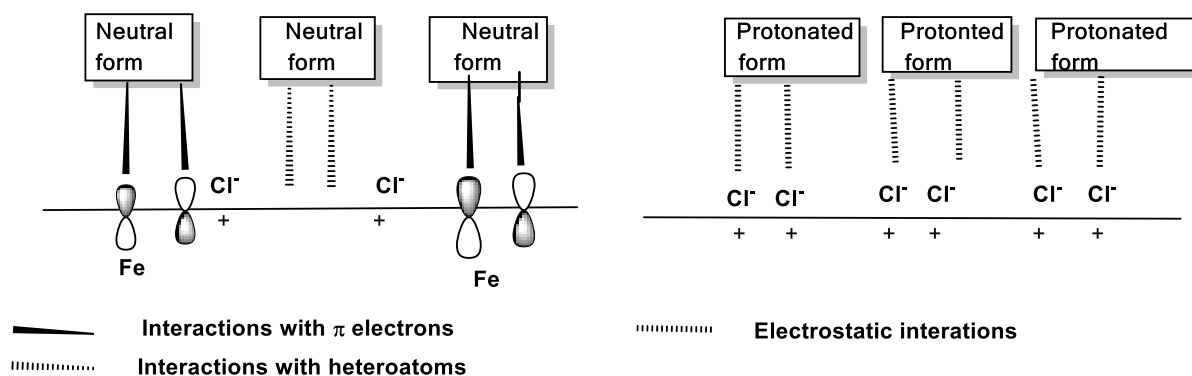
Figure 17. Representation of the different modes of adsorption of Glibenclamide on the CS surface.

5. CONCLUSION

Glibenclamide can effectively inhibit carbon steel degradation in a degradative acid solution. Glibenclamide adsorption fits well with Temkin isotherm. Increasing IE% by higher solution temperatures plus greater Glibenclamide concentration, indicating chemical adsorption of Glibenclamide upon outer layer of CS. Potentiodynamic data suggest Glibenclamide a dual-function inhibitor. Double layer capacitance progressively decreases in presence of Glibenclamide due to formation of safe shield against degradation upon the external layer of CS, unlike Glibenclamide absence. Measured data obtained from electrochemical, non-electrochemical, process and surface examination are accurate and reliable.

6.   REFERENCES

[1]   A. A. Al-Amiery, W. N. R. W. Isahak and W. K. Al-Azzawi, "Corrosion inhibitors: Natural and synthetic organic inhibitors," Lubricants, vol. 11, no. 4, p. 174, 2023.

[2]   I. A. A. Aziz, M. H. Abdulkareem, I. A. Annon, M. M. Hanoon, M. H. Al-Kaabi, L. M. Shaker and M. S. Takriff, "Weight loss, thermodynamics, SEM, and electrochemical studies on N-2-methylbenzylidene-4-antipyrineamine as an inhibitor for mild steel corrosion in hydrochloric acid," Lubricants, vol. 10, no. 2, p. 23, 2022.

[3]   H. W. Lee, M. B. Djukic and C. Basaran, "Modeling fatigue life and hydrogen embrittlement of bcc steel with unified mechanics theory," International Journal of Hydrogen Energy, vol. 48, no. 54, pp. 20773-20803, 2023.

[4]   B. S. Mahdi, M. K. Abbass, M. K. Mohsin, W. K. Al-Azzawi, M. M. Hanoon, M. H. H. Al-Kaabi and M. S. Takriff, "Corrosion inhibition of mild steel in hydrochloric acid environment using terephthaldehyde based on Schiff base: Gravimetric, thermodynamic, and computational studies," Molecules, vol. 27, no. 15, p. 4857, 2022.

[5]   R. K. Mehta, M. Yadav and I. B. Obot, "Electrochemical and computational investigation of adsorption and corrosion inhibition behaviour of 2-aminobenzohydrazide derivatives at mild steel surface in 15% HCl," Materials Chemistry and Physics, vol. 290, no. 1, p. 126666, 2022.

[6] P. Pillai, M. Maiti and A. Mandal, "Mini-review on recent advances in the application of surface-active ionic liquids: petroleum industry perspective," Energy and Fuels, vol. 36, no. 15, pp. 7925-7939, 2022.

[7] O. Dagdag, "An overview of corrosion Anticorrosive Nanomaterials: Future perspectives," Nanomaterials, vol. 56, no. 1, p. 44, 2022.

[8] A. O. Gadioli, L. M. De Souza, E. C. Pereira, S. N. Monteiro and A. R. Azevedo, "Imidazolium-based ionic liquids as corrosion inhibitors for stainless steel in different corrosive media: An overview," Journal of Materials Research and Technology, 2024.

[9] R. Aslam, M. Mobin, S. Zehra and J. Aslam, "A comprehensive review of corrosion inhibitors employed to mitigate stainless steel corrosion in different environments," Journal of Molecular Liquids, vol. 364, no. 1, p. 119992, 2022.

[10] Q. Mohsen and M. A. Deyab, "Utilizing birch leaf extract in pickling liquid as a sustainable source of corrosion inhibitor for pipeline steel," Scientific Reports, vol. 12, no. 1, p. 19307, 2022.

[11] C. Verma, A. Alfantazi, M. A. Quraishi and K. Y. Rhee, "Significance of Hammett and Taft substituent constants on bonding potential of organic corrosion inhibitors: Tailoring of reactivity and performance," Coordination Chemistry Reviews, vol. 495, no. 1, p. 215385, 2023.

[12] A. Zakeri, E. Bahmani and A. S. R. Aghdam, "Plant extracts as sustainable and green corrosion inhibitors for protection of ferrous metals in corrosive media: A mini review," Corrosion Communications, vol. 5, no. 1, pp. 25-38, 2022.

[13] C. S. Proença, B. Serrano, J. Correia and M. E. M. Araújo, "Evaluation of tannins as potential green corrosion inhibitors of aluminium alloy used in aeronautical industry," Metals, vol. 12, no. 3, p. 508, 2022.

[14] M. Gabsi, H. Ferkous, A. Delimi, A. Boublia, C. Boulechfar, A. Kahlouche and Y. Benguerba, "The curious case of polyphenols as green corrosion inhibitors: a review on their extraction, design, and applications," Environmental Science and Pollution Research, vol. 30, no. 21, pp. 59081-59105, 2023.

[15] S. Znaniecki, K. Szwabińska, J. Wojciechowski, A. Skrzypczak and G. Lota, "Ionic liquid modified electrochemical capacitor with long-term performance," ChemElectroChem, vol. 8, no. 19, pp. 3685-3694, 2021.

[16] F. R. Kashani and M. Rezaei, "Improving the localized corrosion resistance of 304 stainless steel in HCl solution by adsorption of molybdate ions: interaction mechanisms at the interface using molecular dynamics simulation and electrochemical noise analysis," Colloids and Surfaces A: Physicochemical and Engineering Aspects, vol. 647, no. 1, p. 129085, 2022.

[17] F. Simescu-Lazar, S. Slaoui, M. Essahli, F. Bohr, A. Lamiri, L. Vanoye and J. P. Chopart, "Thymus satureoides oil as green corrosion inhibitor for 316L stainless steel in 3% NaCl: experimental and theoretical studies," Lubricants, vol. 11, no. 2, p. 56, 2023.

[18] E. K. Ardakani, E. Kowsari, A. Ehsani and S. Ramakrishna, "Performance of all ionic liquids as the eco-friendly and sustainable compounds in inhibiting corrosion in various media: a comprehensive review," Microchemical Journal, vol. 165, no. 1, p. 106049, 2021.

[19] A. K. Bambam, A. Dhanola and K. K. Gajrani, "A critical review on halogen-free ionic liquids as potential metalworking fluid additives," Journal of Molecular Liquids, vol. 380, no. 1, p. 121727, 2023.

[20] F. E. Hajjaji, E. Ech-Chihbi, R. Salim, A. Titi, M. Messali, B. El Ibrahimi, S. Kaya and M. Taleb, "A detailed electronic-scale DFT modeling/MD simulation, electrochemical and surface morphological explorations of imidazolium-based ionic liquids as sustainable and non-toxic corrosion inhibitors for mild steel in 1 M HCl," Materials Science and Engineering: B, vol. 289, no. 1, p. 116232, 2023.

[21] M. A. Tigori, A. V. Kouakou, P. M. Niamien and A. Trokourey, "Inhibition Performance of Some Sulfonylurea on Copper Corrosion in Nitric Acid Solution Evaluated Theoretically by DFT Calculations," Open Journal of Physical Chemistry, vol. 10, no. 3, pp. 139-157, 2020.

[22] R. Ganapathi Sundaram and M. Sundaravadivelu, "Anticorrosion Activity of 8-Quinoline Sulphonyl Chloride on Mild Steel in 1 M HCl Solution," Journal of Metallurgy, vol. 2016, no. 1, Art. no. 8095206, 2016.

[23] P. Singh, M. A. Quraishi and E. E. Ebenso, "Investigation of Gliclazide Drug as Novel Corrosion Inhibitor for Mild Steel in 1 M HCl Solution," International Journal of Electrochemical Science, vol. 7, no. 12, pp. 12270-12282, 2012.

[24] A. S. Fouda, A. M. Eldesoky, M. A. Diab and A. Nabih, "Inhibitive, Adsorption Studies on Carbon Steel Corrosion in Acidic Solutions by New Synthesized Benzene Sulfonamide Derivatives," International Journal of Electrochemical Science, vol. 11, no. 12, pp. 9998-10019, 2016.

[25] N. Vaszilcsin, A. Kellenberger, M. L. Dan, D. A. Duca and V. L. Ordodi, "Efficiency of expired drugs used as corrosion inhibitors: A review," Materials, vol. 16, no. 16, p. 5555, 2023.

[26] P. D. Desai, C. B. Pawar, M. S. Avhad and A. P. More, "Corrosion inhibitors for carbon steel: A review," Vietnam Journal of Chemistry, vol. 61, no. 1, pp. 15-42, 2023.

[27] K. Subbiah, H. S. Lee, M. R. Al-Hadeethi, T. Park and H. Lgaz, "Assessment of the inhibitive performance of a hydrazone derivative for steel rebar in a simulated concrete medium: Establishing the inhibition mechanism at an experimental and theoretical level," Chemical Engineering Journal, vol. 458, no. 1, p. 141347, 2023.

[28] C. Merimi, B. Hammouti, K. Zaidi, B. Hafez, H. Elmsellem, R. Touzani and S. Kaya, "Acetylsalicylic acid as an environmentally friendly corrosion inhibitor for carbon steel XC48 in chloride environment," Journal of Molecular Structure, vol. 1278, no. 1, p. 134883, 2023.

[29] A. M. Salem, A. M. Wahba, A. El Hossiany and A. S. Fouda, "Experimental and computational chemical studies on the corrosion inhibitive properties of metamizole sodium pharmaceutical drug compound for CS in hydrochloric acid solutions," Journal of Industrial and Chemical Society, vol. 99, no. 1, p. 100778, 2022.

[30] S. Shojaee, M. S. Zandi and N. Rastakhiz, "The effect of tetracycline drug as a green corrosion inhibitor for carbon steel in HCl media," Journal of Industrial and Chemical Society, vol. 99, no. 1, p. 100700, 2022.

[31] Z. S. Mahmoud, A. K. Shams and T. A. Salman, "Study the inhibition effect of amoxicillin drug for corrosion of carbon steel in saline media," Baghdad Science Journal, vol. 19, no. 1, p. 0121, 2022.

[32] V. Mehmeti, "Nystatin drug as an effective corrosion inhibitor for mild steel in acidic media-an experimental and theoretical study," Corrosion Science and Technology, vol. 21, no. 1, pp. 21–31, 2022.

[33] M. A. Deyab, O. A. El-Shamy, H. K. Thabet, and A. M. Ashmawy, "Electrochemical and theoretical investigations of favipiravir drug performance as ecologically benign corrosion inhibitor for aluminum alloy in acid solution," Scientific Reports, vol. 13, no. 1, p. 8680, 2023.

[34] F. E. Abeng, M. E. Ikpi, P. C. Okafor, V. C. Anadebe, V. I. Chukwuike, K. J. Uwakwe and N. O. Anaekwe, "Corrosion inhibition of API 5L X-52 pipeline steel in oilfield acidizing solution by gentamicin and sulfamethoxazole: Experimental, plane-wave density functional theory (PWDFT) and the generalized-gradient approximation (GGA) simulations," Journal of Adhesion Science and Technology, vol. 36, no. 22, pp. 2438–2461, 2022.

[35] A. I. Ikeuba, O. B. John, V. M. Bassey, H. Louis, A. U. Agobi, J. E. Ntibi and F. C. Asogwa, "Experimental and theoretical evaluation of aspirin as a green corrosion inhibitor for mild steel in acidic medium," Results in Chemistry, vol. 4, no. 1, p. 100543, 2022.

[36] R. A. Hameed, G. M. Aleid, A. Khaled, D. Mohammad, E. H. Aljuhani, S. R. Al-Mhyawi and M. Abdallah, "Expired dulcolax drug as corrosion inhibitor for low carbon steel in acidic environment," International Journal of Electrochemical Science, vol. 17, no. 6, p. 220655, 2022.

[37] D. A. Duca, M. L. Dan and N. Vaszilcsin, "Expired domestic drug-paracetamol-as corrosion inhibitor for carbon steel in acid media," IOP Conference Series: Materials Science and Engineering, vol. 416, no. 1, p. 012043, 2018.

[38] M. Abdallah, H. Hawsawi, A. S. Al-Gorair, M. T. Alotaibi, S. S. Al-Juaid and R. A. Hameed, "Appraisal of adsorption and inhibition effect of expired micardis drug on aluminum corrosion in hydrochloric acid solution," International Journal of Electrochemical Science, vol. 17, no. 4, p. 220462, 2022.

[39] K. A. Alamry, A. Khan, J. Aslam, M. A. Hussein and R. Aslam, "Corrosion inhibition of mild steel in hydrochloric acid solution by the expired Ampicillin drug," Scientific Reports, vol. 13, no. 1, p. 6724, 2023.

[40] M. Alfakeer, M. Abdallah and A. Fawzy, "Corrosion inhibition effect of expired ampicillin and flucloxacillin drugs for mild steel in aqueous acidic medium," International Journal of Electrochemical Science, vol. 15, no. 1, pp. 3283–3297, 2020.

[41] S. Abd El Maksoud, A. E. A. Fouda and H. Badawy, "Furosemide drug as a corrosion inhibitor for carbon steel in 1.0 M hydrochloric acid," Scientific Reports, vol. 14, no. 1, p. 9052, 2024.

[42] A. S. Fouda, A. A. Ibrahim and W. T. El-behairy, "Thiophene derivatives as corrosion inhibitors for carbon steel in hydrochloric acid solutions," Scholars Research Library, vol. 6, no. 5, pp. 144-157, 2014.

[43] S. M. Shaban, I. Aiad, M. M. El-Sukkary, E. A. Soliman and M. Y. El-Awady, "Evaluation of some cationic surfactants based on dimethylaminopropylamine as corrosion inhibitors," Journal of Industrial and Engineering Chemistry, vol. 21, no. 1, pp. 1029–1038, 2015.

[44] F. Bentiss, M. Lagrenee, M. Traisnel, and J. C. Hornez, "The corrosion inhibition of mild steel in acidic media by a new triazole derivative," Corrosion Science, vol. 41, no. 4, pp. 789-803, 1999.

[45] I. Ahamad and M. A. Quraishi, "Bis (benzimidazol-2-yl) disulphide: An efficient water soluble inhibitor for corrosion of mild steel in acid media," Corrosion Science, vol. 51, no. 9, pp. 2006–2013, 2009.

[46] S. S. Abdel-Rehim, K. F. Khaled, and N. S. Abd-Elshafi, "Electrochemical frequency modulation as a new technique for monitoring corrosion inhibition of iron in acid media by new thiourea derivative," Electrochimica Acta, vol. 51, no. 16, pp. 3269–3277, 2006.

[47] B. Delley, "From molecules to solids with the DMol 3 approach," The Journal of Chemical Physics, vol. 113, no. 18, pp. 7756–7764, 2000.

[48] R. Solmaz, "Investigation of adsorption and corrosion inhibition of mild steel in hydrochloric acid solution by 5-(4-Dimethylaminobenzylidene) rhodanine," Corrosion Science, vol. 79, no. 1, pp. 169–176, 2014.

[49] D. D. N. Singh, R. S. Chaudhary, B. Prakash and C. V. Agarwal, "Inhibitive efficiency of some substituted thioureas for the corrosion of aluminium in nitric acid," British Corrosion Journal, vol. 14, no. 4, pp. 235–239, 1979.

[50] S. K. Shukla and M. A. Quraishi, "4-Substituted anilinomethylpropionate: new and efficient corrosion inhibitors for mild steel in hydrochloric acid solution," Corrosion Science, vol. 51, no. 9, pp. 1990–1997, 2009.

[51] A. S. Fouda, A. A. Al-Sarawy and E. E. El-Katori, "Pyrazolone derivatives as corrosion inhibitors for C-steel in hydrochloric acid solution," Desalination, vol. 201, no. 1-3, pp. 1–13, 2006.

[52] Sh. Masroor and M. Mobin, "Non-Ionic Surfactant as Corrosion Inhibitor for Aluminium in 1 M HCl and Synergistic Influence of Gemini Surfactant," Chemical Science Review and Letters, vol. 3, no. 11S, pp. 33–48, 2014.

[53] A. M. El-desoky, A. S. Fouda and A. Nabih, "Inhibitive, adsorption, synergistic studies on copper corrosion in nitric acid solutions by some organic derivatives," Advanced Material Corrosion, vol. 2, no. 1, pp. 1–15, 2013.

[54] S. G. Lakshmi, S. Tamilselvi, N. Rajendran, M. A. K. Babi and D. Arivuoli, "Electrochemical behavior and characterisation of plasma nitrided Ti–5Al–2Nb–1Ta orthopaedic alloy in Hanks solution," Surface and Coatings Technology, vol. 182, no. 2-3, pp. 287–293, 2004.

[55] X. Li, S. Deng, G. Mu, H. Fu and F. Yang, "Inhibition effect of nonionic surfactant on the corrosion of cold rolled steel in hydrochloric acid," Corrosion Science, vol. 50, no. 2, pp. 420–430, 2008.

[56] A. S. Fouda, D. Mekkia, and A. H. Badr, "Extract of Camellia sinensis as green inhibitor for the corrosion of mild steel in aqueous solution," Journal of the Korean Chemical Society, vol. 57, no. 2, pp. 264–271, 2013.

[57] M. Abdallah, "Rhodanine azosulpha drugs as corrosion inhibitors for corrosion of 304 stainless steel in hydrochloric acid solution," Corrosion Science, vol. 44, no. 4, pp. 717–728, 2002.

[58] I. Ahamad, R. Prasad and M. A. Quraishi, "Thermodynamic, electrochemical and quantum chemical investigation of some Schiff bases as corrosion inhibitors for mild steel in hydrochloric acid solutions," Corrosion Science, vol. 52, no. 3, pp. 933–942, 2010.

[59] M. El Achouri, S. Kertit, H. M. Gouttaya, B. Nciri, Y. Bensouda, L. Perez, M. Infante, and K. Elkacemi, "Corrosion inhibition of iron in 1 M HCl by some gemini surfactants in the series of alkanediyl-α,ω-bis-(dimethyl tetradecyl ammonium bromide)," Progress in Organic Coatings, vol. 43, no. 4, pp. 267–273, 2001.

[60] A. P. Hanza, R. Naderi, E. Kowsari, and M. Sayebani, "Corrosion behavior of mild steel in H2SO4 solution with 1, 4-di [1′-methylene-3′-methyl imidazolium bromide]-benzene as an ionic liquid," Corrosion Science, vol. 107, no. 1, pp. 96-106, 2016.

[61] S. F. Mertens, C. Xhoffer, B. C. Decooman, and E. Temmerman, "Short-term corrosion of polymer-coated 55% Al-Zn-Part 1: Behavior of thin polymer films," Corrosion, vol. 53, no. 3, pp. 381-388, 1997.

[62] E. A. Noor and A. H. Al-Moubaraki, "Thermodynamic study of metal corrosion and inhibitor adsorption processes in mild steel/1-methyl-4[4′(-X)-styrylpyridinium iodides]/hydrochloric acid systems," Materials Chemistry and Physics, vol. 110, no. 1, pp. 145-154, 2008.

[63] R. A. Prabhu, T. V. Venkatesha, A. V. Shanbhag, G. M. Kulkarni and R. G. Kalkhambkar, "Inhibition effects of some Schiff's bases on the corrosion of mild steel in hydrochloric acid solution," Corrosion Science, vol. 50, no. 12, pp. 3356-3362, 2008.

[64] Y. Tang, X. Yang, W. Yang, Y. Chen and R. Wan, "Experimental and molecular dynamics studies on corrosion inhibition of mild steel by 2-amino-5-phenyl-1, 3, 4-thiadiazole," Corrosion Science, vol. 52, no. 1, pp. 242-249, 2010.

[65] G. A. Caignan, S. K. Metcalf and E. M. Holt, "Thiophene substituted dihydropyridines," Journal of Chemical Crystallography, vol. 30, no. 1, pp. 415-422, 2000.

[66] R. Kamaraj, P. Ganesan, J. Lakshmi and S. Vasudevan, "Removal of copper from water by electrocoagulation process-effect of alternating current (AC) and direct current (DC)," Environmental Science and Pollution Research, vol. 20, no. 1, pp. 399-412, 2013.

[67] K. Boumhara, M. Tabyaoui, C. Jama and F. Bentiss, "Artemisia Mesatlantica essential oil as green inhibitor for carbon steel corrosion in 1 M HCl solution: Electrochemical and XPS investigations," Journal of Industrial and Engineering Chemistry, vol. 29, no. 1, pp. 146-155, 2015.

[68] V. S. Sastri, M. Elboujdaini, J. R. Brown and J. R. Perumareddi, "Surface analysis of inhibitor films formed in hydrogen sulfide medium," Corrosion, vol. 52, no. 6, pp. 447-452, 1996.

[69] N. El Hamdani, R. Fdil, M. Tourabi, C. Jama and F. Bentiss, "Alkaloids extract of Retama monosperma (L.) Boiss. seeds used as novel eco-friendly inhibitor for carbon steel corrosion in 1 M HCl solution: Electrochemical and surface studies," Applied Surface Science, vol. 357, no. 1, pp. 1294-1305, 2015.

[70] X. Gao, S. Liu, H. Lu, F. Gao and H. Ma, "Corrosion inhibition of iron in acidic solutions by monoalkyl phosphate esters with different chain lengths," Industrial & Engineering Chemistry Research, vol. 54, no. 7, pp. 1941–1952, 2015.

[71] M. J. Goldberg, J. G. Clabes and C. A. Kovac, "Metal-polymer chemistry. II. Chromium-polyimide interface reactions and related organometallic chemistry," Journal of Vacuum Science & Technology A: Vacuum, Surfaces, and Films, vol. 6, no. 3, pp. 991–996, 1988.

[72] T. Gu, Z. Chen, X. Jiang, L. Zhou, Y. Liao, M. Duan, H. Wang and Q. Pu, "Synthesis and inhibition of N-alkyl-2-(4-hydroxybut-2-ynyl) pyridinium bromide for mild steel in acid solution: Box–Behnken design optimization and mechanism probe," Corrosion Science, vol. 90, no. 1, pp. 118–132, 2015.

[73] B. Senthilvadivu, V. Aswini and K. S. Kumar, "Anti-corrosive behavior of ethanolic extract of banana peel against acidic media and their thermodynamic studies," International Journal of Science, vol. 6, no. 1, pp. 1762–1768, 2007.

[74] M. Yadav, S. Kumar, R. R. Sinha, I. Bahadur and E. E. Ebenso, "New pyrimidine derivatives as efficient organic inhibitors on mild steel corrosion in acidic medium: Electrochemical, SEM, EDX, AFM and DFT studies," Journal of Molecular Liquids, vol. 211, no. 1, pp. 135–145, 2015.

[75] A. Meneguzzi, C. A. Ferreira, M. C. Pham, M. Delamar and P. C. Lacaze, "Electrochemical synthesis and characterization of poly (5-amino-1-naphthol) on mild steel electrodes for corrosion protection," Electrochimica Acta, vol. 44, no. 12, pp. 2149–2156, 1999.

[76] J. Zhang, X. L. Gong, H. H. Yu and M. Du, "The inhibition mechanism of imidazoline phosphate inhibitor for Q235 steel in hydrochloric acid medium," Corrosion Science, vol. 53, no. 10, pp. 3324–3330, 2011.

[77] M. K. Awad, M. S. Metwally, S. A. Soliman, A. A. El-Zomrawy and M. A. Bedair, "Experimental and quantum chemical studies of the effect of polyethylene glycol as corrosion inhibitors of aluminum surface," Journal of Industrial and Engineering Chemistry, vol. 20, no. 3, pp. 796–808, 2014.

[78] A. Dehghani, G. Bahlakeh and B. Ramezanzadeh, "Green Eucalyptus leaf extract: a potent source of bio-active corrosion inhibitors for mild steel," Bioelectrochemistry, vol. 130, no. 1, p. 107339, 2019.

[79] K. Zhang, W. Yang, X. Yin, Y. Chen, Y. Liu, J. Le and B. Xu, "Amino acids modified konjac glucomannan as green corrosion inhibitors for mild steel in HCl solution," Carbohydrate Polymers, vol. 181, no. 1, pp. 191–199, 2018.

[80] E. Berdimurodov, A. Kholikov, K. Akbarov, L. Guo, S. Kaya, D. K. Verma, M. Rbaa and O. Dagdag, "Novel glycoluril pharmaceutically active compound as a green corrosion inhibitor for the oil and gas industry," Journal of Electroanalytical Chemistry, vol. 907, no. 1, p. 116055, 2022.